

Article

Effect of Ammonium Chloride on the Efficiency with Which Copper Sulfate Activates Marmatite: Change in Solution Composition and Regulation of Surface Composition

Shengdong Zhang, Dongxia Feng, Xiong Tong *, Bo Yang and Xian Xie *

Faculty of Land Resource Engineering, Kunming University of Science and Technology, Kunming 650000, China; Kmustzhangsd@126.com (S.Z.); dongxia.feng@uqconnect.edu.au (D.F.); boyang2012@sohu.com (B.Y.)

* Correspondence: kgxiongtong@163.com (X.T.); xianxie2008@kmust.edu.cn (X.X.)

Received: 14 May 2018; Accepted: 11 June 2018; Published: 13 June 2018



Abstract: Zinc sulfide minerals are the primary choice for zinc extraction and marmatite is one of the two most common zinc sulphide minerals (sphalerite and marmatite), therefore it is of great significance to study and optimize the flotation of marmatite. To improve the activation of copper sulfate on marmatite, a method involving the addition of ammonium chloride is devised. The method has been proven to be an effective way of improving the activation efficiency of copper sulfate towards marmatite under alkaline conditions. The strengthening mechanism was studied using micro-flotation, adsorption test, X-ray photoelectron spectroscopy, and by analyzing changes in solution composition. Flotation test results show that the activation effect of the copper sulfate towards marmatite is enhanced with the addition of ammonium chloride. According to the results of the adsorption measurements and X-ray photoelectron spectroscopy analysis, when the marmatite surface is activated using copper sulfate with added ammonia chloride, it adsorbs more copper sulfide and less copper hydroxide and zinc hydroxide. These changes in surface composition are believed to occur via the following process: $\text{NH}_3(\text{aq})$ promotes the dissolution of zinc hydroxide and then facilitates the conversion of surface copper hydroxide to copper sulfide. In addition, the occurrence of $\text{Cu}(\text{NH}_3)_n^{2+}$ can promote the adsorption of copper ions (Cu^{2+} can be stored as $\text{Cu}(\text{NH}_3)_n^{2+}$ via complexation, and then, when the concentration of copper ions decreases, Cu^{2+} can be released through the decomposition of $\text{Cu}(\text{NH}_3)_n^{2+}$. Hence, the copper ion concentration can be maintained and this can facilitate the adsorption of Cu^{2+} on marmatite). Based on a comprehensive analysis of all our results, we propose that adding ammonium chloride to the copper sulfate changes the solution components (i.e., the presence of $\text{NH}_3(\text{aq})$ and $\text{Cu}(\text{NH}_3)_n^{2+}$) and then regulates the surface composition of marmatite. The change in surface composition improves the hydrophobicity of mineral surface and this leads to an improvement in activation of marmatite.

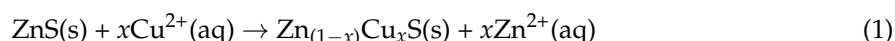
Keywords: marmatite; activation; cuprammonium ion; flotation

1. Introduction

Zinc is an important metal resource with significant application value in many industrial areas [1]. Compared to zinc oxide minerals, zinc sulfide minerals (sphalerite and marmatite) remain the primary source of zinc because the beneficiation technology used to extract zinc from them is economically and technically advantageous [2,3]. However, zinc sulfide minerals are commonly associated with pyrite in mineral deposits. Thus, the separation of sphalerite or marmatite from pyrite is a problem that must be faced during the beneficiation of zinc sulfide minerals [4].

As the pyrite surface is hydrophilic in alkaline conditions [5–7], separation is usually achieved by depressing pyrite in alkaline environment [8–11]. Zinc sulfide minerals have poor affinities towards xanthate and so they are usually activated using copper sulfate before being collected using xanthate. However, when the pyrite is depressed in alkaline conditions, the activation of sphalerite or marmatite using copper sulfate is also affected. This is because, in alkaline media, copious amounts of copper hydroxide are formed in the copper sulfate solution at the concentrations generally used (10^{-6} to 10^{-4} mol/L) [12–17].

The formation of copper hydroxide leads to two significant changes. First, the copper ion concentration is kept low, which means that the activation of zinc sulfide mineral through the ion-exchange process (as shown by Equation (1)) is weakened [18–24]. Secondly, the activation effect caused by copper sulfide converted from adsorbed copper hydroxide (as shown by Equations (2) and (3)) becomes dominant [19–21]:



The floatability of the zinc sulfide minerals after activation is determined by the ratio of surface hydrophobic species (such as copper sulfides, polysulfides, and elemental sulfur) and hydrophilic species (such as hydroxides) [25]. As the process of transformation of copper hydroxide into copper sulfide is related to the dissolution of surface zinc hydroxide, the transformation process is relatively slow [18]. Therefore, when the copper sulfate concentration is excessively high, the copper hydroxide adsorbed on the mineral surface cannot be completely transformed into copper sulfide within a limited activation time. As a result, the ratio of hydrophilic copper hydroxide on the mineral surface is increased and will result in the depression of the zinc sulfide minerals. Flotation experiments on zinc sulfide minerals (and related surface detection experiments) reported by Boulton [14], Mirnezami [26], and Fornasiero et al. [20] all confirm that excessively high concentrations of copper sulfate under alkaline conditions cause depression of zinc sulfide minerals because of the adsorption of large amounts of copper hydroxide.

The problem of activating zinc sulfide minerals using copper sulfate under alkaline conditions stems from defects in the activation process related to copper hydroxide formation. The activation mechanism when using CuSO_4 in alkaline environments has some flaws: (1) the activation rate is affected by the dissolution of zinc hydroxide on the mineral surface; and (2) the activation effect is sensitive to the copper concentration [18,20].

Therefore, it makes sense to consider taking measures to mitigate the above-mentioned effects and strengthen the activation effect of copper sulfate on zinc sulfide minerals under alkaline conditions. Some research has already been done in this area. One method in particular, adding ammonium chloride, has been used to enhance the activation of copper sulfate towards marmatite under alkaline conditions [27,28]. However, these studies have merely verified the feasibility of the method—no attempts were made to investigate the mechanisms involved in great depth. Therefore, in this paper, research is carried out on the mechanism by which ammonium chloride strengthens the activation of marmatite using copper sulfate under alkaline conditions. Micro-flotation, adsorption test, X-ray photoelectron spectroscopy (XPS), and copper-concentration measurements are the tools used to accomplish this.

2. Experimental

2.1. Materials and Reagents

The marmatite sample used in this study was obtained from the Dulong Mine in Yunnan Province, China. The sample was dry-ground using a porcelain ball mill and then dry-screened to select particles

of size 0.075 ± 0.044 mm for experimental use. The chemical composition of the sample is presented in Table 1. The marmatite sample was stored in a glass bottle and protected under N_2 . In all experiments, the marmatite samples were first scrubbed under ultrasonication for 5 min and then washed three times with deionized water to obtain fresh, consistent, mineral surfaces.

Table 1. The chemical composition of the marmatite used in this study.

	Component							
	Zn	S	Fe	Pb	Cu	Si	CaO	MgO
Content (%)	57.18	32.41	8.51	0.15	0.039	1.27	0.15	0.12

All the water used was purified using an ultra-pure water machine (UPT-I-10T, ULUPURE, Xi'an, China) with a (RO) reverse osmosis unit. The specific resistance of the Milli-Q water is $18.2 \text{ M}\Omega \cdot \text{cm}^{-1}$. The copper sulfate ($\text{CuSO}_4 \cdot 5\text{H}_2\text{O}$), ammonium chloride (NH_4Cl), sodium hydroxide (NaOH), and ethylenediaminetetraacetic acid disodium salt (disodium EDTA) used in the experiments were all of analytical purity. The collector, sodium isobutyl xanthate, was purified by dissolving it in acetone and then recrystallizing it from ether. A fresh sample was prepared in solution on the day of use to avoid oxidation and decomposition.

2.2. Flotation Experiments

Flotation experiments were conducted in a 50 mL Hallimond tube with 1 g of marmatite sample (0.075 ± 0.044 mm) per test. After being scrubbed under ultrasonication for 5 min and then washed three times with deionized water, the marmatite sample was first conditioned for 4 min in the tube with 40 mL of pH = 9 (adjusted by 0.001 mol/L NaOH) activator solution with desired concentration. It was then conditioned for another 2 min with addition of 4 mg/L of sodium isobutyl xanthate. After that, flotation was performed for 10 min with an air flow rate of 0.010 L/min. After flotation was finished, the floated and non-floated fractions were filtered, dried at 40°C , and then weighed to calculate recovery. Each test was repeated three times and the average recovery rate calculated for final reporting. The experimental errors of recovery are quantified using standard deviation.

2.3. Adsorption Tests

The residual concentration method was used to measure the total amount of copper adsorbed. Extraction with disodium EDTA was used to achieve selective extraction and determine the amount of copper hydroxide adsorbed onto the marmatite surface.

A sample (1 g) of marmatite after washing was first conditioned in 20 mL corresponding pH = 9 (adjusted by 0.001 mol/L NaOH) activator solution (3×10^{-5} mol/L CuSO_4 /cuprammonium solution (3×10^{-5} mol/L CuSO_4 plus 6×10^{-4} mol/L NH_4Cl)) for a required amount of time. After conditioning, the suspension was filtered and the filtrate was stored in a waterless and clean tube as "Sample No. 1" for testing—the filter residue was quickly transferred to a 50 mL waterless and clean vial for extraction. The extraction was conducted in 20 mL 3 wt % disodium EDTA solution for 20 min. After the extraction was complete, the suspension was filtered and the filtrate was stored in a waterless and clean tube as "Sample No. 2" for testing. The disodium EDTA solution was purged with nitrogen before use to reduce the oxygen content of the solution to prevent oxidation of the marmatite during the extraction process. Extraction was performed at pH = 9 (adjusted by 0.001 mol/L NaOH) to ensure a good extraction effect was obtained [29].

The copper and zinc concentration was measured using inductively coupled plasma atomic emission spectrometry (ICP-AES) (ICPS-1000II, Shimadzu, Kyoto, Japan). The sample to be tested is acidified with hydrochloric acid before testing to prevent hydrolysis and precipitation of metal

ions. The total amount of copper adsorbed and the extracted and unextracted copper on the marmatite surface can be calculated using the following expressions:

$$\Gamma_{\text{total}} = (C_0 - C_1)V_1/M \quad (4)$$

$$\Gamma_{\text{extracted}} = C_2V_2/M \quad (5)$$

$$\Gamma_{\text{unextracted}} = \Gamma_{\text{total}} - \Gamma_{\text{extracted}} \quad (6)$$

where C_0 , C_1 , and C_2 are the initial copper concentration, the copper concentration of Sample No. 1, and that of Sample No. 2, respectively. The volumes V_1 and V_2 are the volume of the activation solution used for treatment and the disodium EDTA solution used for extraction, respectively, and M is the mass of the solid sample used in each adsorption test.

The extracted zinc can also be calculated using the Formula (5). However, in this case, C_2 is the zinc concentration of Sample No. 2.

The experimental errors of adsorption amount are quantified through standard deviation and are presented in the graph.

2.4. XPS Analysis

To compare the composition of the material produced on marmatite surface conditioned with copper sulfate solution and that conditioned with cuprammonium solution, XPS measurements were undertaken. The XPS measurements were carried out using a spectrometer (PHI5000 Versaprobe II, ULVAC-PHI, CHIGASAKI-SHI, Kanagawa, Japan) equipped with a monochromatic Al K X-ray source at a pass-energy of 46.95 eV. The pressure in the analyzer chamber was 5×10^{-9} mba during analysis. The detection process included a survey scan to identify the chemical components present and high-resolution scans to detect the levels of certain elements.

First of all, 1 g of washed marmatite was stirred for 10 min with the following solutions, respectively (each at pH = 9):

- (a) Deionized water,
- (b) 6×10^{-4} mol/L NH_4Cl ,
- (c) 3×10^{-5} mol/L CuSO_4 ,
- (d) 3×10^{-5} mol/L $\text{CuSO}_4 + 3 \times 10^{-4}$ mol/L NH_4Cl ,
- (e) 3×10^{-5} mol/L $\text{CuSO}_4 + 6 \times 10^{-4}$ mol/L NH_4Cl .

After being conditioned, the suspension was filtered and then the filter residue was rinsed with deionized water three times. After flushing, these samples were dried in a vacuum drying oven at 30 °C. After drying, these samples were correspondingly labeled "(a)–(e)" and their XPS spectra were recorded.

2.5. Concentration of Copper in Solution

The 3×10^{-5} mol/L copper sulfate solution and cuprammonium solutions with different molar ratios of ammonium chloride to copper sulfate were prepared. Then, all solutions were adjusted to pH = 9 and centrifuged at 3000 rpm (using a TL4.7W centrifuge, Shanghai Shengkalan Industrial Co., Ltd., Shanghai, China) for 30 min. After that, the solutions were filtered by the syringe filter (the pore size of the filter is 0.22 μm) and the copper concentrations of filtrates were measured using ICP-AES.

3. Results

3.1. Flotation Results

At pH = 9, under the condition of 4 mg/L sodium isobutyl xanthate and a fixed $M(\text{NH}_4\text{Cl})/M(\text{CuSO}_4)$ of cuprammonium solution, the flotation experiments with and without addition of ammonium chloride were conducted and the results are shown in Figure 1.

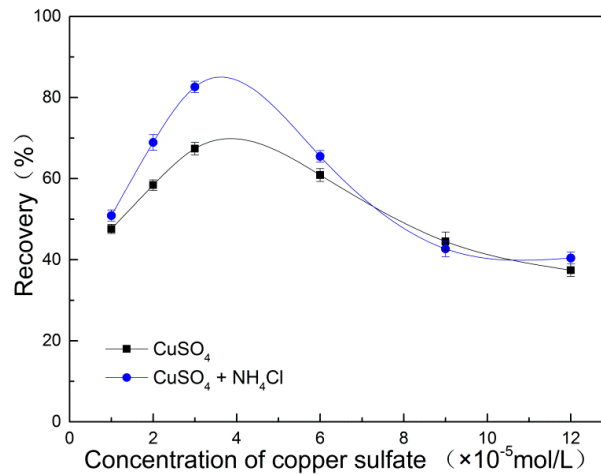


Figure 1. Flotation recovery rate of marmatite as a function of copper sulfate concentration (pH = 9, C (sodium isobutyl xanthate) = 4 mg/L, $M(\text{NH}_4\text{Cl})/M(\text{CuSO}_4) = 20$).

As shown in Figure 1, when the copper sulfate concentration in the range of $2\sim 6 \times 10^{-5}$ mol/L, the recovery is significantly higher when the copper sulfate has ammonium chloride added to it. When the copper sulfate concentration exceeds 6×10^{-5} mol/L, the recovery rates with and without addition of NH_4Cl both show a downwards trend, in agreement with previous research [14,20,26]. This is expected to be due to the marmatite surface being coated with copper hydroxide formed in the presence of excessive amounts of copper sulfate under mild alkaline conditions.

To further explore the effect of adding ammonium chloride on the activation of marmatite by copper sulfate, the flotation rate experiment under activation of 3×10^{-5} mol/L CuSO_4 and 3×10^{-5} mol/L $\text{CuSO}_4 + 6 \times 10^{-4}$ mol/L NH_4Cl are conducted, the experimental results are shown in Figure 2.

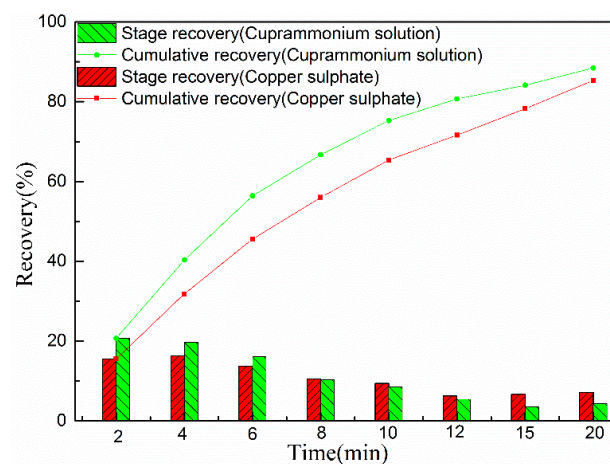


Figure 2. Cumulative and stage flotation recovery of marmatite activated using copper sulphate (3×10^{-5} mol/L CuSO_4) and cuprammonium solution (3×10^{-5} mol/L $\text{CuSO}_4 + 6 \times 10^{-4}$ mol/L NH_4Cl). (pH = 9, C (sodium isobutyl xanthate) = 4 mg/L).

Figure 2 shows that the addition of ammonium chloride leads to an increase in flotation rate during the first six minutes of flotation. The flotation results clearly show that adding ammonium chloride improves the flotation rate of marmatite.

3.2. Adsorption Test Results

3.2.1. Copper Adsorption

The amount of copper adsorbed is a parameter that allows us to intuitively assess the activation effect of the mineral. According to previous research [12,19,20], the copper adsorbed onto the surface of the sphalerite and marmatite when they are activated by copper sulfate under alkaline conditions usually appears in the form of both copper sulfides and copper hydroxide. Obviously, these different copper compounds will have a completely different effect on the hydrophobicity of the mineral surface. Therefore, the activation effect cannot be properly characterized by simply measuring the total amount of copper adsorbed onto the surface of the mineral.

Rumball et al. [29] found that disodium EDTA can be used to selectively leach metal oxides, hydroxides, carbonates, and sulfates from sulfide minerals. Fornasiero and Gerson [12,20] used disodium EDTA to extract copper hydroxide from the surface of sphalerite in their research on how copper sulfate activates the sphalerite. The selective extraction effect of the disodium EDTA was verified in their research using XPS.

In order to separately determine the amounts of copper sulfide and copper hydroxide adsorbed onto the marmatite surface, selective extraction of the adsorbed copper hydroxide component was carried out using disodium EDTA. Under alkaline conditions (pH = 9), the amounts of copper sulfide and copper hydroxide adsorbed on the marmatite after conditioning in 3×10^{-5} mol/L copper sulfate, with and without the addition of ammonium chloride, were measured and compared as a function of time (Figure 3).

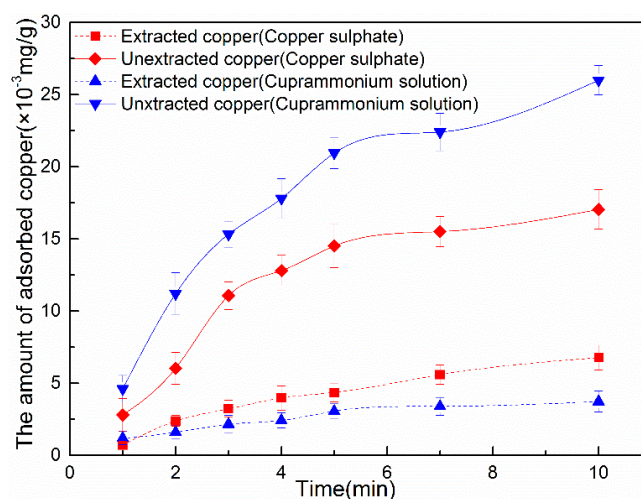


Figure 3. The amount of unextracted (sulfide) and extracted (hydroxide) copper adsorbed onto the marmatite conditioned in copper sulphate (3×10^{-5} mol/L CuSO_4) and cuprammonium solution (3×10^{-5} mol/L $\text{CuSO}_4 + 6 \times 10^{-4}$ mol/L NH_4Cl) as a function of conditioning time (pH = 9).

In Figure 3, the unextracted copper corresponds to copper sulfide and the extracted copper corresponds to copper hydroxide. As the figure shows, the amount of copper hydroxide and copper sulfide adsorbed increase with time in both of the two solutions. For a given amount of conditioning time, it is clear that the addition of ammonium chloride leads to a significantly larger amount of copper sulfide adsorbed onto the marmatite compared to conditioning using just copper sulfate. As for the

hydroxide component, the addition of ammonium chloride clearly suppresses the amount of copper hydroxide formed over time.

3.2.2. Zinc Hydroxide Adsorption

The method of EDTA extraction was also used to extract the surface adsorbed zinc hydroxide, and the results are presented in Figure 4.

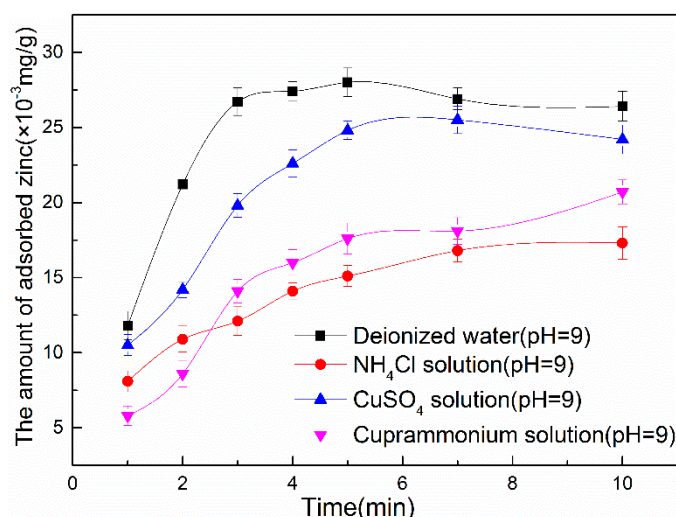


Figure 4. The amount of zinc hydroxide adsorbed on surface of marmatite conditioned in (I) deionized water; (II) 6×10^{-4} mol/L NH_4Cl ; (III) 3×10^{-5} mol/L CuSO_4 ; (IV) 3×10^{-5} mol/L $\text{CuSO}_4 + 6 \times 10^{-4}$ mol/L NH_4Cl , respectively (pH = 9), as a function of conditioning time.

As the figure shows, compared with marmatite treated in deionized water, less zinc hydroxide adsorbed on the surface of marmatite conditioned in NH_4Cl ; Compared with marmatite treated in 3×10^{-5} mol/L CuSO_4 , zinc hydroxide adsorbed on the surface of marmatite conditioned in cuprammonium solution (3×10^{-5} mol/L $\text{CuSO}_4 + 6 \times 10^{-4}$ mol/L NH_4Cl) decreases with increasing ammonia chloride addition. It can be concluded from these results that adding NH_4Cl can reduce zinc hydroxide adsorbed on marmatite surface.

3.3. XPS Studies

To explore the differences occurring in marmatite surfaces conditioned in copper sulfate, with and without the addition of ammonium chloride, marmatite samples conditioned in different solutions were subjected to XPS analysis.

The XPS spectra and surface atomic ratios of sample “(a)–(e)” were obtained and calculated based on the Multi-Pak Spectrum software (V 9.0). The C1s spectral peak at 284.8 eV was used for calibration of all spectra. The XPS survey scan results are listed in Table 2.

Table 2. XPS survey scan results of marmatite sample conditioned in solutions (a)–(e), respectively.

Sample	Atomic Concentration (%)					
	C 1s	O 1s	S 2p	Fe 2p	Zn 2p	Cu 2p
a	29.57	29.45	19.80	2.80	18.38	0.00
b	32.48	18.35	24.03	3.62	21.52	0.00
c	30.23	22.93	19.80	2.46	14.92	9.66
d	34.47	16.53	19.91	2.59	15.46	11.04
e	31.61	14.48	22.14	2.76	16.50	12.51

From the above table, it can be seen that the most obvious changes in surface content occurred on oxygen and copper and no significant change in the content of other elements was found. Whether in the case of deionized water treatment or copper sulfate treatment, the oxygen content on the mineral surface shows a significant drop after the addition of ammonium chloride. The drop in surface oxygen content may result from decreased content of surface-adsorbed hydroxide. In the case of conditioning in copper sulphate, the amount of copper adsorbed on the mineral surface increases with the increase in the amount of ammonium chloride added. The results obtained from the XPS survey scan results are consistent with the EDTA extraction results, which proves the reliability of XPS analysis to some extent.

3.3.1. Surface Nitrogen Analysis

Figure 5 shows the N 1s XPS spectra of samples “(c)–(e)”. It can be seen from the figure that the N 1s XPS spectra of the three samples are all similar and lack obvious peaks at band energies of 398.60 eV (NH_3) [30] and 401.80 eV (NH_4^+) [31] or other positions. This means that none of these samples contained significant amounts of NH_3 and NH_4^+ or other nitrogenous substances, such as $\text{Cu}(\text{NH}_3)_n^{2+}$, on the surfaces of the particles contained within. This result excludes the possibility that the marmatite is activated through the adsorption of NH_3 , NH_4^+ , or $\text{Cu}(\text{NH}_3)_n^{2+}$.

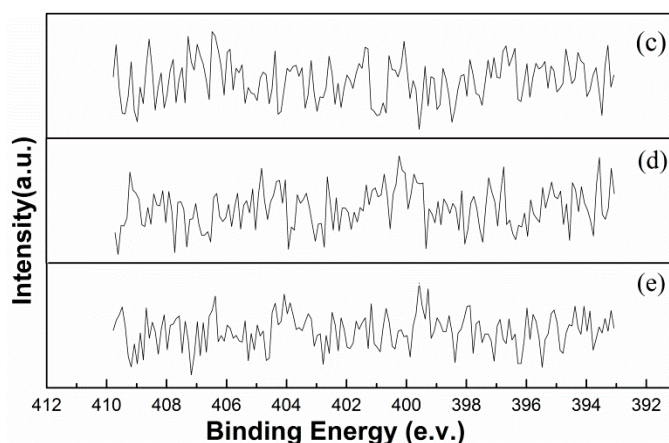


Figure 5. The N 1s XPS spectra of marmatite conditioned using solutions (c)–(e), respectively.

3.3.2. Surface Zinc Analysis

Based on the Zn $2p_{3/2}$ binding energies given in the literature [32–34], the following three zinc species were identified on the surface of the samples: ZnO (1021.20 eV), ZnS (1022.00 eV), and Zn(OH)₂ (1022.70 eV). The ZnO component is probably formed by the dehydration of zinc hydroxide during the drying process [35]. The results of peak fitting of the Zn $2p_{3/2}$ data are shown in Figure 6 and the zinc content is summarized in Table 3.

Table 3. Binding energies and relative contents of the different zinc species occurring on the surface of marmatite conditioned in solutions (a)–(e), respectively.

Sample	Binding Energy (eV)			Total Amount of Zn Present (%)		
	Zn in ZnO	Zn in ZnS	Zn in Zn(OH) ₂	As ZnO	As ZnS	As Zn(OH) ₂
a	1021.18	1022.03	1022.67	50.53	24.75	24.72
b	1021.23	1021.96	1022.65	31.42	60.21	8.38
c	1021.28	1021.94	1022.63	30.43	39.38	30.18
d	1021.14	1022.06	1022.77	28.05	54.69	17.26
e	1021.11	1022.12	1022.79	24.34	58.13	17.53

Compared to sample (a), the ZnO and Zn(OH)₂ content of sample (b) is significantly lower (the total reduction amounts are 35.46%). Comparing the ZnO and Zn(OH)₂ content of samples (c)–(e), wherein increasing amounts of NH₄Cl are added to the copper sulfate, the amounts of ZnO and Zn(OH)₂ present are seen to decrease. The characterization and comparison of the surface zinc species given above shows that adding ammonium chloride does reduce the zinc hydroxide content of the marmatite surface. These results are consistent with the adsorption results given in Section 3.2.2.

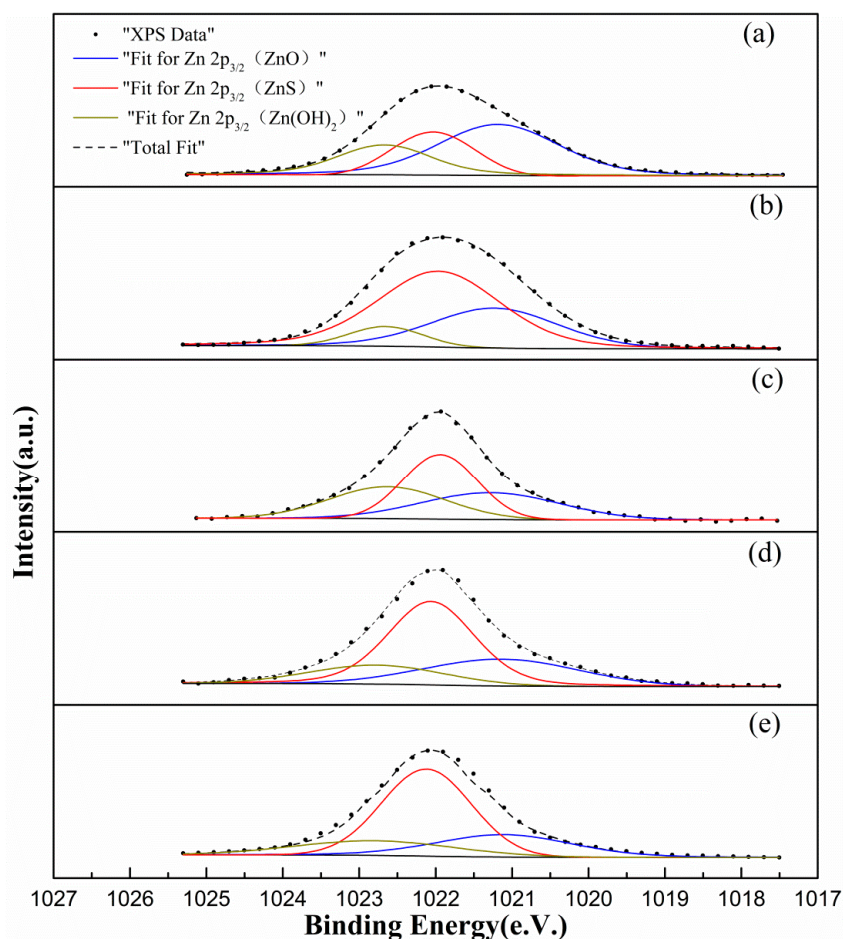


Figure 6. Zn 2p_{3/2} XPS spectra of marmatite conditioned using solutions (a–e), respectively.

3.3.3. Surface Copper Analysis

According to the Cu 2p_{3/2} binding energies given in the literature [36,37], the following three copper species can be identified on the surface of the samples: Cu₂S (932.20 eV), CuO (933.60 eV), and CuS (935.00 eV). The CuO may be formed through the dehydration of the adsorbed copper hydroxide during the vacuum-drying process [38]. The Cu₂S is generated via the reduction of CuS, according to the results of previous research [39]. The peak fitting results for the Cu 2p_{3/2} XPS data are shown in Figure 7 and the corresponding copper content is listed in Table 4.

Table 4. Binding energies and relative copper content on the surface of marmatite conditioned in solutions (c)–(e), respectively.

Sample	Binding Energy (eV)			Total Amount of Cu Present (%)		
	Cu in Cu ₂ S	Cu in CuO	Cu in CuS	As Cu ₂ S	As CuO	As CuS
c	932.19	933.57	934.96	79.35	16.57	4.07
d	932.20	933.65	934.98	88.71	8.28	3.01
e	932.17	933.56	935.00	90.52	3.95	5.53

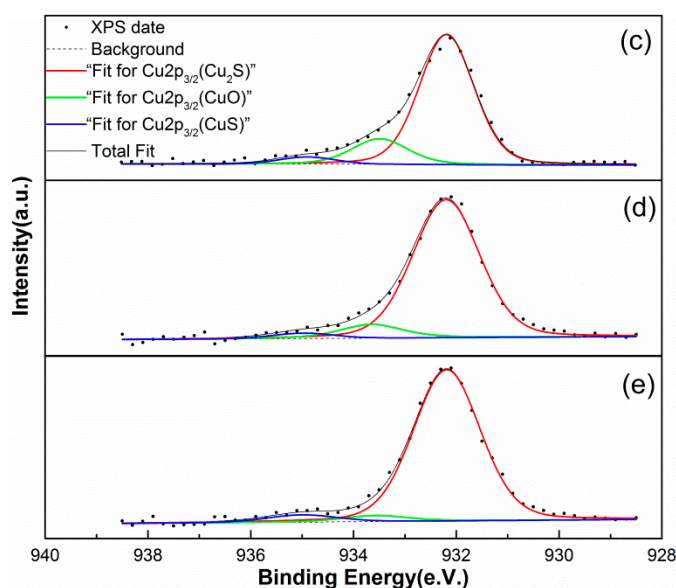


Figure 7. The Cu 2p_{3/2} XPS spectra of marmatite conditioned using solutions (c–e), respectively.

According to previous XPS research [40], the Cu(II) peaks in the Cu 2p XPS spectra should show strong satellite peaks at 943.4 and 961.9 eV. As can be seen from Figure 8, these satellite peaks are all weak and gradually decline in significance from sample (c) to sample (e). This indicates that there is only a small amount of Cu(II) on the surfaces of these samples, which is consistent with the abundances listed in Table 4.

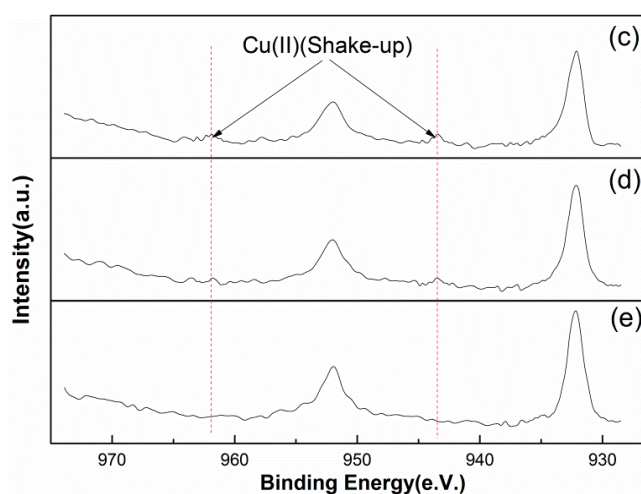


Figure 8. Cu(II) satellite peaks in the Cu 2p XPS spectra of marmatite conditioned in solutions (c)–(e), respectively.

Comparing the copper content of the samples, it can be seen that the relative amount of CuO present gradually decreases as the amount of NH₄Cl added to the copper sulfate increases. The foregoing XPS analysis of the copper species on the mineral surfaces shows that adding NH₄Cl to the copper sulfate reduces the amount of copper hydroxide on the marmatite surface. These results are consistent with the adsorption results given in Section 3.2.1.

3.4. Solution Components

The composition of the solution directly affects adsorption onto the mineral and products formed thereon. Thus, it is a crucial aspect of the flotation process. The differences in the composition of copper sulfate solution, with and without ammonium chloride, will therefore have a significant impact on the activation of the marmatite. Hence, it makes sense to explore the difference in compositions of the two solutions.

Under alkaline conditions (pH = 9), the copper concentration of a copper sulfate solution (3×10^{-5} mol/L) with different amounts of NH₄Cl added were measured. The results are shown in Table 5.

Table 5. Copper concentrations in copper sulfate solutions with different amounts of NH₄Cl added.

Molar Ratio of NH ₄ Cl:CuSO ₄	Measured Copper Concentration (mg/L)
0	0.0506
10	0.0675
20	0.0796
50	0.0972
100	0.1078
200	0.1215

As can be seen from Table 5, for a given pH and copper sulfate concentration, the copper concentration increases as the amount of ammonium chloride added increases. The concentrations listed in Table 4 are all less than the copper concentration corresponding to 3×10^{-5} mol/L (1.91 mg/L), which implies that all the solutions contain copper hydroxide precipitate.

In order to help our discussion of the effect of adding ammonium chloride to the copper sulfate solution, the compositions of s copper sulfate solutions with addition of different amounts of NH₄Cl were calculated using Visual MINTEQ, a chemical equilibrium model frequently used in related fields to calculate metal speciation, solubility equilibria, adsorption, etc. in aqueous solution [41–45]. The latest version (3.1) was used in this work.

Under alkaline conditions (pH = 9), and with a copper sulfate concentration of 3×10^{-5} mol/L, the results of the equilibrium calculations when different amounts of NH₄Cl are present are shown in Figure 9. It can be seen from the figure that, as the amount of NH₄Cl increases, the proportion of dissolved copper increases. This is consistent with the results of our copper concentration measurements. More specifically, the activities of the Cu(NH₃)_n²⁺, CuCl[−], and CuCl₂(aq) components all increase while the activities of the other copper-containing components are almost unchanged. Considering the greater magnitudes of the activities of the Cu(NH₃)_n²⁺ species (compared to CuCl[−] and CuCl₂(aq)), these ions are believed to be the ones responsible for the increase in the copper concentration as NH₄Cl is added.

The experimental results, combined with the solution chemistry calculations, show that, at pH = 9, the concentration of Cu²⁺ in both systems (3×10^{-5} mol/L CuSO₄ and cuprammonium solution consisting of 3×10^{-5} mol/L CuSO₄ + 6×10^{-4} mol/L NH₄Cl) at equilibrium are determined by the solubility product K_{sp} of Cu(OH)₂(s). The significant difference between these two systems is that part of the copper hydroxide is dissolved to form Cu(NH₃)_n²⁺ in the cuprammonium solution.

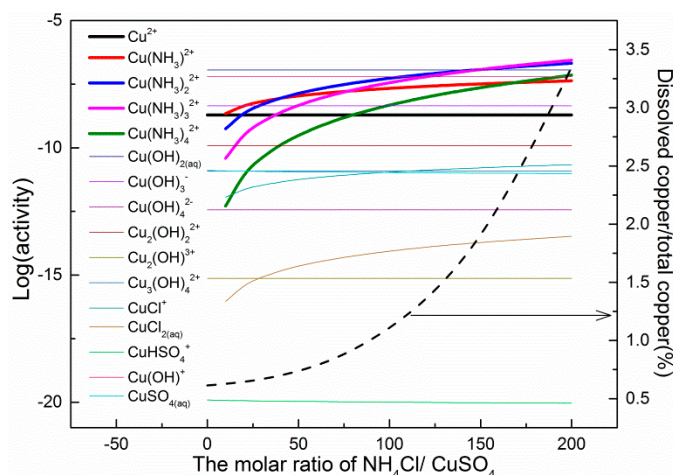
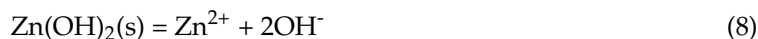
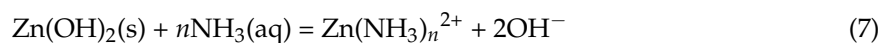


Figure 9. Calculated activities of the components of copper/ammonium solutions of different molar ratio ($\text{NH}_4\text{Cl}:\text{CuSO}_4$) under alkaline conditions ($\text{pH} = 9$) and with $[\text{CuSO}_4] = 3 \times 10^{-5}$ mol/L. The curves relating to Cu^{2+} and $\text{Cu}(\text{NH}_3)_n^{2+}$ are drawn using bold lines for clarity.

4. Discussion

The XPS analysis and EDTA extraction of the zinc species on the mineral surfaces has confirmed that adding NH_4Cl to the copper sulfate can reduce the amount of zinc hydroxide formed on the marmatite surface. The theoretical explanation for this phenomenon is suggested to be: the $\text{NH}_3(\text{aq})$ can promote the dissolution of the zinc hydroxide through a complexation reaction between NH_3 and Zn^{2+} .

The dissolution of $\text{Zn}(\text{OH})_2(\text{s})$, with and without the involvement of $\text{NH}_3(\text{aq})$, can be represented by the equations:



Equation (7) can be obtained by combining Equations (8) and (9), and so the equilibria constants are such that:

$$K_7 = K_8 \times K_9 \text{ or } K_7/K_8 = K_9$$

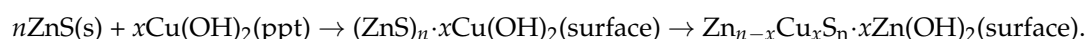
The complexation reactions of Zn^{2+} and NH_3 are listed in Table 6, which shows that the constants corresponding to K_9 are large. Hence, $K_7 \gg K_8$. This comparison of equilibria constants theoretically justifies the enhancement effect of $\text{NH}_3(\text{aq})$ on the dissolution of zinc hydroxide.

Table 6. Zinc-ammonia complexation reactions and corresponding equilibrium constants (from Ref. [46]).

Equilibrium	$\log K^a$
$\text{Zn}^{2+} + \text{NH}_3 \rightleftharpoons \text{Zn}(\text{NH}_3)^{2+}$	2.35
$\text{Zn}^{2+} + 2\text{NH}_3 \rightleftharpoons \text{Zn}(\text{NH}_3)_2^{2+}$	4.80
$\text{Zn}^{2+} + 3\text{NH}_3 \rightleftharpoons \text{Zn}(\text{NH}_3)_3^{2+}$	7.31
$\text{Zn}^{2+} + 4\text{NH}_3 \rightleftharpoons \text{Zn}(\text{NH}_3)_4^{2+}$	9.46

^a At 25 °C and 100,000 Pa.

According to previous studies [19–21,39], the activation of zinc sulfide minerals under alkaline conditions is mainly achieved through the following process:



The Zn(OH)_2 formed on the marmatite surface during activation will undergo dissolution and dispersion, the extent of which affects the copper hydroxide replacement process. This then determines the degree of hydrophobicity of the marmatite surface.

The copper adsorption measurements in Section 3.2 and copper XPS analysis of the surface species in Section 3.3.3 both indicate that adding NH_4Cl to the copper sulfate solution leads to a reduction in the amount of copper hydroxide on the marmatite surface. In addition to the reactions replacing the copper hydroxide on the surface, the reduction in surface copper hydroxide could also be due to the promotion of zinc hydroxide dissolution, which accelerates the reactions replacing the copper hydroxide. In the copper adsorption measurements, the amount of copper hydroxide increased more slowly (and copper sulfide increased more rapidly) on the surface of marmatite conditioned using copper sulfate with added ammonium chloride, which coincides with this explanation.

In accordance with the above discussion, the following mechanism can be hypothesized. Adding ammonium chloride to the copper sulfate solution promotes the dissolution of zinc hydroxide on the marmatite surface and then facilitates the transformation of adsorbed copper hydroxide into a stable activation product (copper sulfide). This causes an increase in the amount of surface copper sulfide, which can easily adsorb thiol collectors and decreases the amount of hydrophilic zinc hydroxide and copper hydroxide on the surface. The combination of these two effects eventually results in a significant increase in the recovery of marmatite during flotation.

Further analysis of the copper adsorption results reveals a noteworthy phenomenon: The amount of copper sulfide present increases much faster than the rate at which the amount of copper hydroxide decreases when conditioned with copper sulfate and ammonium chloride (compared with copper sulfate on its own).

The above phenomenon and the observed differences in the solutions' components suggests that there may be another mechanism occurring simultaneously: the $\text{Cu(NH}_3)_n^{2+}$ formed after adding ammonium chloride has the effect of storing and releasing Cu^{2+} —hence, it can “buffer” the tendency of the copper ion concentration to drop and then promote the Cu^{2+} adsorption process.

Although precipitated copper hydroxide is the main form of copper under alkaline conditions, a certain amount of the Cu^{2+} remains in solution which is still able to activate the marmatite through the copper-zinc ion-exchange mechanism [18–21].

Regardless of which solution is used (copper sulfate or cuprammonium solution), during the absorption of copper ions onto the marmatite surface, there is continuous shifting of the dynamic equilibria between the components of the solution. In the cuprammonium solution, the Cu^{2+} equilibrium processes occurring during the adsorption process can be represented by the simplified scheme shown in Figure 10.

Several aspects of the processes illustrated in Figure 10 are in need of further explanation: (1) in the diagram, $C_2 < C_{\text{saturated}}$. The reason for this is that the copper hydroxide has not yet decomposed to release and replenish the Cu^{2+} concentration and so the total copper concentration is reduced due to the adsorption of copper ions onto the mineral surface; (2) the $\text{Cu(NH}_3)_n^{2+}$ ions are uniformly dispersed in the liquid phase, while the copper hydroxide exists as a precipitate or colloid in the solid state [27]. Thus, the contact area between the former and the marmatite surface is much greater than that of the latter. When copper ions are adsorbed onto the mineral surface, the decrease in copper ion concentration will initially affect the dissociation equilibria of the $\text{Cu(NH}_3)_n^{2+}$ species in the liquid phase. The dissolution equilibrium of the copper hydroxide will be affected until the fall in copper concentration spreads to the liquid phase near the solid surface of the copper hydroxide. Therefore, when the concentration of Cu^{2+} decreases, $\text{Cu(NH}_3)_n^{2+}$ will decompose before the copper hydroxide decomposes.

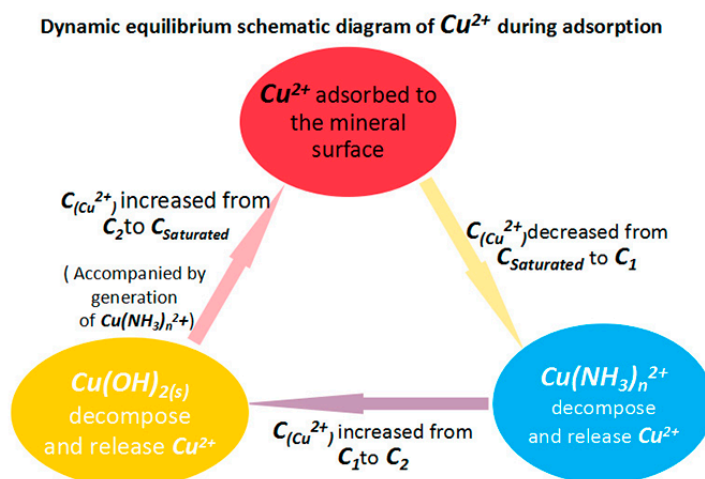


Figure 10. Schematic diagram of the dynamic equilibria affecting the Cu^{2+} concentration during adsorption. The Cu^{2+} concentrations featured are: $C_{\text{saturated}}$ is the saturated value determined by the solubility product K_{sp} of $\text{Cu}(\text{OH})_2(\text{s})$; C_1 is that after copper ion adsorption but before $\text{Cu}(\text{NH}_3)_n^{2+}$ decomposition; C_2 is the concentration after $\text{Cu}(\text{NH}_3)_n^{2+}$ decomposition but before $\text{Cu}(\text{OH})_2(\text{s})$ decomposition.

As can be seen from the processes shown in Figure 10, $\text{Cu}(\text{NH}_3)_n^{2+}$ has the function of storing and releasing Cu^{2+} . It can maintain the concentration of Cu^{2+} and thereby accelerates the adsorption of Cu^{2+} .

5. Conclusions

In this work, the mechanism by which ammonium chloride enhances the activation of marmatite by copper sulfate has been theoretically analyzed based on the results of micro-flotation experiments, adsorption tests, XPS analysis, and a comparison of the components of the solutions. A model for this mechanism can thus be established, as shown in Figure 11.

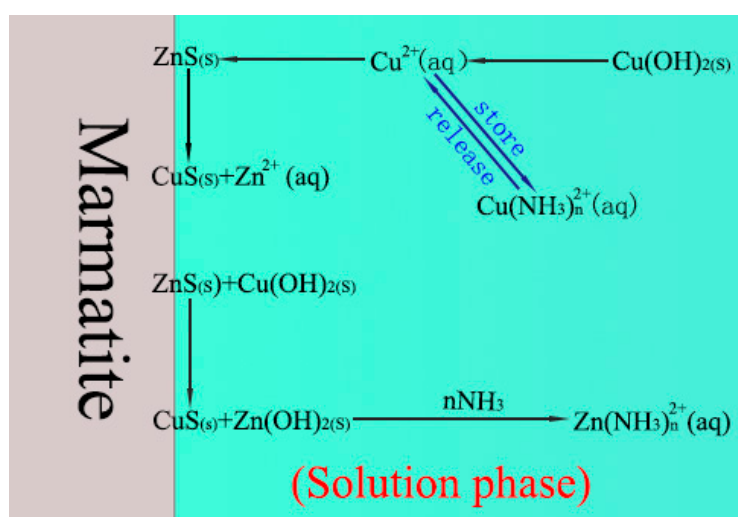


Figure 11. Schematic diagram showing how NH_4Cl enhances the activation of marmatite by copper sulfate.

The main conclusions of the paper can be described using this model, as follows:

- (1) The addition of NH_4Cl to the copper sulfate results in a significant change in the composition of the solution (critically, it causes the presence of $\text{NH}_3(\text{aq})$ and $\text{Cu}(\text{NH}_3)_n^{2+}$). These changes subsequently lead to the regulation of the surface composition of the marmatite.
- (2) Aqueous ammonia, $\text{NH}_3(\text{aq})$, promotes the dissolution of zinc hydroxide on the marmatite surface through the formation of zinc–ammonia complex ions and then promotes the conversion of copper hydroxide to copper sulfide on the mineral surface. This increases the amount of copper sulfide on the surface, and also significantly reduces the hydrophilic hydroxide content of the surface, thereby enhancing the activation effect.
- (3) The $\text{Cu}(\text{NH}_3)_n^{2+}$ species buffer the copper ion concentration by storing and releasing copper ions (and hence resists large drops in Cu^{2+} ion concentration). This effect helps facilitate the adsorption of copper ions and formation of copper sulfide and finally promotes the activation effect.

Author Contributions: X.T. and X.X. conceived and designed the experiments; S.Z. and B.Y. performed the experiments; S.Z., D.F., X.T., B.Y. and X.X. analyzed the data; S.Z. wrote this paper; and D.F. corrected it.

Acknowledgments: The authors would like to acknowledge the funding provided by the National Natural Science Foundation of China (No. 51764024 and No. 51764025) and Analysis and Testing Foundation of Kunming University of Science and Technology (No. 2016M20152101097).

Conflicts of Interest: The authors declare they have no conflicts of interest.

References

1. Mudd, G.M.; Jowittl, S.M.; Werner, T.T. The world's lead–zinc mineral resources: Scarcity, data, issues and opportunities. *Ore Geol. Rev.* **2017**, *80*, 1160–1190. [[CrossRef](#)]
2. Irannajad, M.; Ejtemaei, M.; Gharabaghi, M. The effect of reagents on selective flotation of smithsonite-calcite-quartz. *Miner. Eng.* **2009**, *22*, 766–771. [[CrossRef](#)]
3. Kashani, A.N.; Rashchi, F. Separation of oxidized zinc minerals from tailings: Influence of flotation reagents. *Miner. Eng.* **2008**, *21*, 967–972. [[CrossRef](#)]
4. Mu, Y.; Peng, Y.; Lauten, R.A. The depression of pyrite in selective flotation by different reagent systems—A Literature review. *Miner. Eng.* **2016**, *96–97*, 143–156. [[CrossRef](#)]
5. Rao, S.R.; Leja, J. *Surface Chemistry of Forth Flotation: Reagents and Mechanisms*; Springer: New York, NY, USA, 2004; p. 223.
6. Boulton, A.; Fornasiero, D.; Ralston, J. Characterisation of sphalerite and pyrite flotation samples by XPS and ToF–SIMS. *Int. J. Miner. Process.* **2003**, *70*, 205–219. [[CrossRef](#)]
7. He, S.; Fornasiero, D.; Skinner, W. Correlation between copper-activated pyrite flotation and surface species: effect of pulp oxidation potential. *Miner. Eng.* **2005**, *18*, 1208–1213. [[CrossRef](#)]
8. Zhang, Q.; Xu, Z.; Bozkurt, V.; Finch, J.A. Pyrite flotation in the presence of metal ions and sphalerite. *Int. J. Miner. Process.* **1997**, *52*, 187–201. [[CrossRef](#)]
9. Shen, W.Z.; Fornasiero, D.; Ralston, J. Effect of collectors, conditioning pH and gases in the separation of sphalerite from pyrite. *Miner. Eng.* **1998**, *11*, 145–158. [[CrossRef](#)]
10. Dichmann, T.K.; Finch, J.A. The role of copper ions in sphalerite–pyrite flotation selectivity. *Miner. Eng.* **2001**, *14*, 217–225. [[CrossRef](#)]
11. Finch, J.A.; Rao, S.R.; Nessel, J.E. Iron control in mineral processing. In Proceedings of the 39th Annual Meeting of the Canadian Mineral Processors of CIM, Ottawa, ON, Canada, 23–25 January 2007.
12. Lascelles, D.; Sui, C.C.; Finch, J.A.; Butler, I.S. Copper ion mobility in sphalerite activation. *Colloids Surf. A Physicochem. Eng. Asp.* **2001**, *186*, 163–172. [[CrossRef](#)]
13. Weisener, C.; Gerson, A. An investigation of the Cu (II) adsorption mechanism on pyrite by ARXPS and SIMS. *Miner. Eng.* **2000**, *13*, 1329–1340. [[CrossRef](#)]
14. Boulton, A.; Fornasiero, D.; Ralston, J. Effect of iron content in sphalerite on flotation. *Miner. Eng.* **2005**, *18*, 1120–1122. [[CrossRef](#)]
15. Duarte, A.C.P.; Grano, S.R. Mechanism for the recovery of silicate gangue minerals in the flotation of ultrafine sphalerite. *Miner. Eng.* **2007**, *20*, 766–775. [[CrossRef](#)]

16. Huang, G.; Grano, S. Galvanic interaction of grinding media with pyrite and its effect on flotation. *Miner. Eng.* **2005**, *18*, 1152–1163. [[CrossRef](#)]
17. Khmeleva, T.N.; Skinner, W.; Beattie, D.A. Depressing mechanisms of sodium bisulphite in the collectorless flotation of copper-activated sphalerite. *Int. J. Miner. Process.* **2005**, *76*, 43–53. [[CrossRef](#)]
18. Finkelstein, N.P. The activation of sulphide minerals for flotation: A review. *Int. J. Miner. Process.* **1997**, *52*, 81–120. [[CrossRef](#)]
19. Gerson, A.R.; Lange, A.G.; Prince, K.E.; Smart, R.S.C. The mechanism of copper activation of sphalerite. *Appl. Surf. Sci.* **1999**, *137*, 207–223. [[CrossRef](#)]
20. Fornasiero, D.; Ralston, J. Effect of surface oxide/hydroxide products on the collectorless flotation of copper-activated sphalerite. *Int. J. Miner. Process.* **2006**, *78*, 231–237. [[CrossRef](#)]
21. Prestidge, C.A.; Skinner, W.M.; Ralston, J.; Smart, R.S.C. Copper (II) activation and cyanide deactivation of zinc sulphide under mildly alkaline conditions. *Appl. Surf. Sci.* **1997**, *108*, 333–344. [[CrossRef](#)]
22. Buckley, A.N.; Skinner, W.M.; Harmer, S.L.; Pring, A.; Lamb, R.N.; Fan, L.J.; Yang, Y.W. Examination of the proposition that Cu (II) can be required for charge neutrality in a sulfide lattice-Cu in tetrahedrites and sphalerite. *Can. J. Chem.* **2007**, *85*, 767–781. [[CrossRef](#)]
23. Viñals, J.; Fuentes, G.; Hernández, M.C.; Herreros, O. Transformation of sphalerite particles into copper sulfide particles by hydrothermal treatment with Cu (II) ions. *Hydrometallurgy* **2004**, *75*, 177–187. [[CrossRef](#)]
24. Chen, Z.; Yoon, R.H. Electrochemistry of copper activation of sphalerite at pH 9.2. *Int. J. Miner. Process.* **2000**, *58*, 57–66. [[CrossRef](#)]
25. Ralston, J.; Healy, T.W. Activation of zinc sulphide with CuII, CdII and PbII: II. Activation in neutral and weakly alkaline media. *Int. J. Miner. Process.* **1980**, *7*, 203–217. [[CrossRef](#)]
26. Mirnezami, M.; Restrepo, L.; Finch, J.A. Aggregation of sphalerite: Role of zinc ions. *J. Colloid Interface Sci.* **2003**, *259*, 36–42. [[CrossRef](#)]
27. Tong, X.; Song, S.; He, J.; Rao, F.; Lopez-Valdivieso, A. Activation of high-iron marmatite in froth flotation by ammoniacal copper(II) solution. *Miner. Eng.* **2007**, *20*, 259–263. [[CrossRef](#)]
28. Xie, X.; Hou, K.; Yang, B.; Tong, X. Activation of sphalerite by ammoniacal copper solution in froth flotation. *J. Chem.* **2016**, *2016*, 7614890. [[CrossRef](#)]
29. Rumball, J.A.; Richmond, G.D. Richmond. Measurement of oxidation in a base metal flotation circuit by selective leaching with disodium EDTA. *Int. J. Miner. Process.* **1996**, *48*, 1–20. [[CrossRef](#)]
30. Peden, C.H.F.; Rogers, J.W., Jr.; Shinn, N.D.; Kidd, K.B.; Tsang, K.L. Thermally grown Si₃N₄ thin films on Si (100): Surface and interfacial composition. *Phys. Rev. B* **1993**, *47*, 15622. [[CrossRef](#)]
31. Sano, T.; Mera, N.; Kanai, Y.; Nishimoto, C.; Tsutsui, S.; Hirakawa, T.; Negishi, N. Origin of visible-light activity of N-doped TiO₂ photocatalyst: Behaviors of N and S atoms in a wet N-doping process. *Appl. Catal. B Environ.* **2012**, *128*, 77–83. [[CrossRef](#)]
32. Kim, S.H.; Kim, H.K.; Seong, T.Y. Electrical characteristics of Pt Schottky contacts on sulfide-treated n-type ZnO. *Appl. Phys. Lett.* **2005**, *86*, 022101. [[CrossRef](#)]
33. Deroubaix, G.; Marcus, P. X-ray photoelectron spectroscopy analysis of copper and zinc oxides and sulphides. *Surf. Interface Anal.* **1992**, *18*, 39–46. [[CrossRef](#)]
34. Pradhan, D.; Leung, K.T. Controlled growth of two-dimensional and one-dimensional ZnO nanostructures on indium tin oxide coated glass by direct electrodeposition. *Langmuir* **2008**, *24*, 9707–9716. [[CrossRef](#)] [[PubMed](#)]
35. Piva, D.H.; Piva, R.H.; Rocha, M.C.; Dias, J.A.; Montedo, O.R.K.; Malavazi, I.; Morelli, M.R. Antibacterial and photocatalytic activity of ZnO nanoparticles from Zn(OH)₂, dehydrated by azeotropic distillation, freeze drying, and ethanol washing. *Adv. Powder Technol.* **2017**, *28*, 463–472. [[CrossRef](#)]
36. Nefedov, V.I.; Salyn, Y.V.; Solozhenkin, P.M.; Pulatov, G.Y. X-ray photoelectron study of surface compounds formed during flotation of minerals. *Surf. Interface Anal.* **1980**, *2*, 170–172. [[CrossRef](#)]
37. Nakamura, T.; Tomizuka, H.; Takahashi, M.; Hoshi, T. Methods of Powder Sample Mounting and Their Evaluations in XPS Analysis. *Hyomen Kagaku* **1995**, *16*, 515–520. [[CrossRef](#)]
38. Ghotbi, M.Y.; Rahmati, Z. Nanostructured copper and copper oxide thin films fabricated by hydrothermal treatment of copper hydroxide nitrate. *Mater. Des.* **2015**, *85*, 719–723. [[CrossRef](#)]
39. Chandra, A.P.; Gerson, A.R. A review of the fundamental studies of the copper activation mechanisms for selective flotation of the sulfide minerals, sphalerite and pyrite. *Adv. Colloid Interface Sci.* **2009**, *145*, 97–110. [[CrossRef](#)] [[PubMed](#)]

40. Li, F.; Zhong, H.; Xu, H.; Jia, H.; Liu, G. Flotation behavior and adsorption mechanism of α -hydroxyoctylphosphinic acid to malachite. *Miner. Eng.* **2015**, *71*, 188–193. [[CrossRef](#)]
41. Sierra, J.; Roig, N.; Papiol, G.G.; Pérez-Gallego, E.; Schuhmacher, M. Prediction of the bioavailability of potentially toxic elements in freshwaters. Comparison between speciation models and passive samplers. *Sci. Total Environ.* **2017**, *605–606*, 211–218. [[CrossRef](#)] [[PubMed](#)]
42. Zuo, M.; Renman, G.; Gustafsson, J.P.; Renman, A. Phosphorus removal performance and speciation in virgin and modified argon oxygen decarburisation slag designed for wastewater treatment. *Water Res.* **2015**, *87*, 271–281. [[CrossRef](#)] [[PubMed](#)]
43. Jia, G.; Zhang, H.; Krampe, J.; Muster, T.; Gao, B.; Zhu, N.; Jin, B. Applying a chemical equilibrium model for optimizing struvite precipitation for ammonium recovery from anaerobic digester effluent. *J. Clean. Prod.* **2017**, *147*, 297–305. [[CrossRef](#)]
44. Sjöstedt, C.; Löf, Å.; Olivecrona, Z.; Boye, K.; Kleja, D.B. Improved geochemical modeling of lead solubility in contaminated soils by considering colloidal fractions and solid phase EXAFS speciation. *Appl. Geochem.* **2018**, *92*, 110–120. [[CrossRef](#)]
45. Crutchik, D.; Sánchez, A.; Garrido, J.M. Simulation and experimental validation of multiple phosphate precipitates in a saline industrial wastewater. *Sep. Purif. Technol.* **2013**, *118*, 81–88. [[CrossRef](#)]
46. *IUPAC Stability Constants Database, Sc-Database and Mini-Scdatabase*, Timble; Academic Software: Otley, UK, 2001.



© 2018 by the authors. Licensee MDPI, Basel, Switzerland. This article is an open access article distributed under the terms and conditions of the Creative Commons Attribution (CC BY) license (<http://creativecommons.org/licenses/by/4.0/>).